International Journal of Heat and Mass Transfer 52 (2009) 2205–2214

Contents lists available at ScienceDirect

International Journal of Heat and Mass Transfer

journal homepage: www.elsevier.com/locate/ijhmt

Configuration of the micro-layer and characteristics of heat transfer in a narrow gap mini/micro-channel boiling system

Yoshio Utaka [a,*], Shuhei Okuda [b], Yutaka Tasaki [c]

[a] Faculty of Engineering, Yokohama National University, Tokiwadai, Hodogaya, Yokohama, Kanagawa 240-8501, Japan
[b] Honda Engineering Co., Ltd., Haga-gun, Tochigi 321-3395, Japan
[c] Nissan Motor Co., Ltd., Natsushima-cho, Yokosuka-shi, Kanagawa 237-8523, Japan

ARTICLE INFO

Article history:
Received 9 April 2008
Received in revised form 29 October 2008
Available online 5 February 2009

Keywords:
Phase change
Boiling
Narrow gap
Mini/micro-channel
Micro-layer thickness
Laser extinction method

ABSTRACT

Heat transfer measurements were performed in a mini/micro-channel boiling system for water, and the thickness of the micro-layer that formed between the heating surface and the generated vapor under vapor growth was measured by application of the laser extinction method for narrow gaps of 0.5, 0.3 and 0.15 mm. The process of bubble growth was recorded by using a high-speed camera simultaneously. The effects of gap size, the velocity of vapor bubble forefront and the distance from the incipient bubble site were investigated on the micro-layer thickness in a narrow gap mini/micro-channel boiling system and the configuration of the thin liquid micro-layer distributions on the heat transfer surface was clarified. Furthermore, factors that would possibly affect the mechanism and characteristics of heat transfer, such as the position of the generated vapor bubble, the velocity of the vapor forefront, the micro-layer dominant period and the liquid saturation period in the boiling cycle, and so forth, were quantitatively investigated and analyzed on the basis of the measured data. The heat transfer characteristics were analyzed and the data calculated were coincided with the measured data in the boiling curve for the gap size of 0.5 and 0.25 mm measured in the previous report. It was shown that the heat transfer was enhanced due to the micro-layer evaporation.

1. Introduction

Recently, the researches and applications on the microscopic phenomena are of great interest. One of the examples in the field of heat transfer with phase change is mini/micro-channel type vapor generator for a fuel cell vehicle with a reformer. A fuel cell vehicle with a reformer requires a high efficiency of heat exchange and low heat capacity to meet power train requirements and realize fast response and compactness. The use of a narrow gap mini/micro-channel vapor generator for a reformer with a large surface area per unit volume and small heat capacity is one possible approach to satisfy these requirements. Since several definitions of "mini" and "micro" [1,2] were presented depending on the hydraulic diameter of other non-dimensional variables and the size of the channel used in this study span both, the term of mini/micro is put to use in this study. The mini/micro-channel refers to that section of the bulk liquid in a plate-shaped vapor generator with thin gaps between the heating plates, as shown in Fig. 1. In the boiling process, the bulk liquid, superheated micro-layer and the bubbles generally affect the boiling characteristics in complicated ways. In particular, in the case of a restricted flow path such as a mini/micro-channel, vapor bubbles have a depressed shape, because they are pushed and crushed by the heating plates and rapidly spread over the heating plates. Therefore, the rate of evaporation at the micro-layer between the plates and the bubbles plays an important role in determining the heat transfer rate.

There have been many investigations on mini/micro-channels. Kandlikar [2] studied the behavior of flow caused by a pressure drop between the inlet and outlet in a horizontal micro-channel with a cross-section of 1×1 mm. Wen et al. [3] studied the heat transfer coefficient of a vertical micro-channel with a cross-section of 1 mm by 2 mm, and a vertical pipe ranging in diameter from 0.8 to 1.7 mm. Thome et al. [4] and Dupont et al. [5] presented a three-zone flow boiling model formulated to describe evaporation of elongated bubbles in micro-channels and is compared to experimental data on the basis of micro-layer evaporation was principal form of heat transfer. For the boiling in narrow gap mini/micro-channels, Katto and Yokoya [6] and Fujita et al. [7] reported that the evaporation characteristics in a mini/micro-channel with a reduced gap size formed by a flat heating surface are completely different from those of pool boiling.

On the other hand, studies on the thin film that forms between the heating surface and bubble in nucleate pool boiling have been performed. For example, Cooper et al. [8] measured the change in the heating surface temperature and calculated the thin film thick-

* Corresponding author. Tel./fax: +81 45 339 3909.
E-mail address: utaka@ynu.ac.jp (Y. Utaka).

0017-9310/$ - see front matter © 2008 Elsevier Ltd. All rights reserved.
doi:10.1016/j.ijheatmasstransfer.2008.11.020

Nomenclature

A	extinction coefficient
D	distance from incipient bubble site
H	height of heat transfer surface
I	detected laser intensity with liquid-layer
I_0	detected laser intensity without liquid-layer
L	latent heat of vaporization
N_B	number of times of initial micro-layer appearance by bubble growth in a bubble period
N_R	number of times of micro-layer appearance by liquid slug in a bubble period
q	average heat flux
s	gap size
t	time
t	time after formation of micro-layer
t_L	term filled with bulk liquid
t_M	term with micro-layer
T	liquid temperature
T_0	vapor saturation temperature
T_W	temperature of heat transfer surface
T_{WE}	final temperature in term with micro-layer
$\Delta T = T_W - T_0$	superheat of heat transfer surface
V	rate of decrease of micro-layer thickness
V_L	local bubble forefront velocity
W	width of heat transfer surface
$x^*=x/H$	non-dimensional height of heat transfer surface
$y^*=y/W$	non-dimensional width of heat transfer surface
z	axis of gap thickness
α	thermal diffusivity
δ	micro-layer thickness
δ_0	initial micro-layer thickness
ρ_L	density
λ	thermal conductivity

ness from the experimental results using an ideal analytical model. Recently, some attempts (Stephan [9] and Wayner [10]) have been made to elucidate the mechanism of heat and mass transfer by precisely modeling the thin film, taking into account the adsorbed liquid film in which intermolecular forces are influential. Comparison with practical cases is still insufficient, and it is important to accumulate experimental results for a variety of boiling systems.

In a previous report, Tasaki and Utaka [11] described observations of the aspects of vapor behavior and heat transfer measurements in the mini/micro-channel for water. The effects of the gap size between the heating plates and the wettability of the heating surface of a mini/micro-channel on the heat transfer characteristics were experimentally studied. It was pointed out that the heat transfer characteristics are mainly governed by these factors. In the case of a gap size between 0.25 and 10 mm, wettability was changed from hydrophilic to hydrophobic by applying coatings of titanium oxide and silicon resin to the lapped copper heating surfaces. The effects of surface wettability on the boiling curve were investigated by observing various factors that affect boiling. It was found that hydrophilic surfaces reduced heat transfer with a 10 mm gap size. On the other hand, with a gap size between 0.25 mm and 1.0 mm, heat transfer was enhanced. It was concluded that the enhancement of heat transfer was due to the formation and sustaining of a micro-liquid-layer on the heating plate with a highly wettable surface.

Two regions are seen for boiling or vaporization in the mini/micro-channel, namely a micro-layer-dominant region and a dryout region as shown in Fig. 2. The open and closed symbols denote the micro-layer-dominant region and the dryout region, respectively. Intermittent formation of the micro-layer, due to the generation of vapor bubble, is observed in the first region. In the other region, periodic forward and backward movements of the liquid at the entrance of the channel, and the appearance of dryout at the exit are observed. For all cases of a gap size of less than 0.5 mm, the maximum heat flux occurs in the dryout region. However, the micro-layer-dominant region occupies approximately 70–80% of the maximum heat flux. Hence, it is seen that the micro-layer-dominant region represents the principal form of heat transfer for mini/micro-channel boiling. For instance, in the region of relatively low superheat, a narrower gap size results in a higher heat transfer coefficient. However, with increasing superheat, the change tends to have an opposite trend. Therefore, clarification of the behavior of the micro-layer is a very important factor in elucidating the mechanism and characteristics of boiling heat transfer in a mini/micro-channel vaporizer.

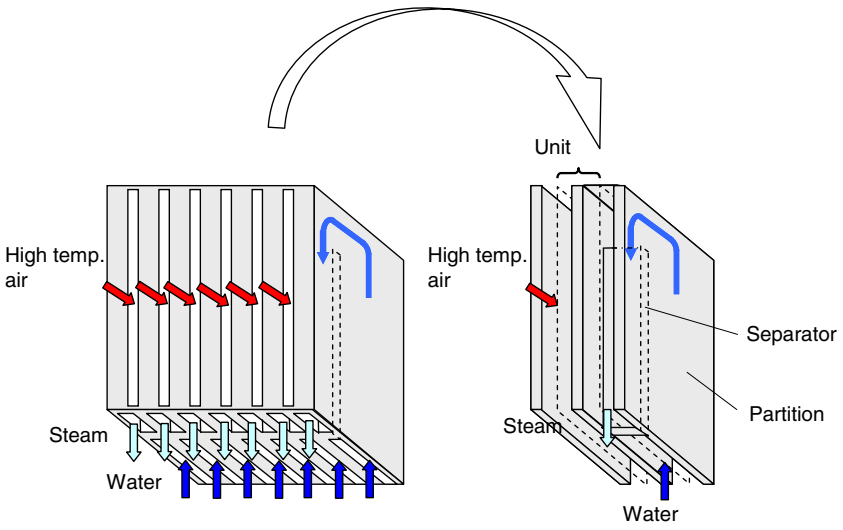

Fig. 1. Mini/micro-channel vapor generator.

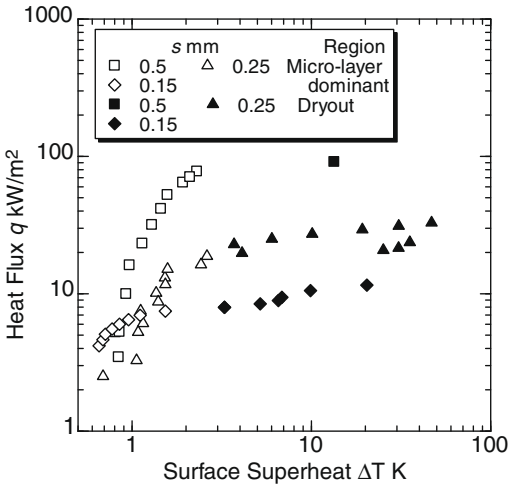

Fig. 2. Effect of gap sizes on boiling curves on titanium oxide-coated surface.

In this study, the characteristics of the micro-layer that forms in the mini/micro-channel vapor generator between the heat transfer surface and bubbles generated during boiling were clarified by the application of high response and non-contact laser extinction method to measure the micro-layer thickness for water. Such a measurement applying the laser extinction characteristics to the thickness measurement of thin liquid film is carried out for Marangoni condensation by Utaka and Nishikawa [12]. Furthermore, the mechanism and characteristics of heat transfer was quantitatively analyzed by investigating factors such as the position of the generated vapor bubble, velocity of vapor forefront, the micro-layer dominant period and the liquid saturation period in the boiling cycle, and so forth, on the basis of the heat transfer measurements, observations of the aspect of boiling given, and the configuration of the micro-layer.

2. Experimental apparatus and method

Fig. 3(a) shows the experimental apparatus consisting of a boiling section in the mini/micro-channel vapor generator, and a section for measuring the micro-layer thickness by application of the laser extinction method. The vapor generator is located between a laser emitter and a detector. The apparatus of mini/micro-channel boiling system is the same as that used in the previous study [11], with the exception of the mini/micro-channel section. A water reservoir and heating tank were placed upstream in the mini/micro-channel test apparatus. The cross-sectional area of the water reservoir was large enough to maintain a constant water level in the mini/micro-channel. The water supplied to the mini/micro-channel apparatus was boiled in a heating tank that was open to the atmosphere. Vapor generated from the mini/micro-channel vapor generator and the heating tank flowed through a condenser and back to the water reservoir. Fig. 3(b) shows the details of the mini/micro-channel test apparatus. Quartz glass with a high transparency for infrared light was mainly utilized for the test apparatus to enable more accurate measurements. Two quartz glass plates form the mini/micro-channel, which is filled with water as the test fluid. Passages for high temperature air used as the heating fluid to heat the mini/micro-channel were positioned at the back and front of the mini/micro-channel. The central part of the 82 mm high passage, which essentially served as the heating area, was narrowed to enhance heating. The width of the passage was 45 mm. The heat flux into the mini/micro-channel was controlled by varying the air temperature from 110 to 300 °C. A cavity of 30 μm diameter was located 12 mm below the center of the mini/micro-channel to provide an incipient bubble site on the heating plate. Two thermocouples to measure the heat flux were embedded at different depths in the quartz glass at points 12 mm above and below the center, respectively.

The contact angle of pure water on the quartz glass heating plates was 26° and the real gap size of the narrower mini/micro-channel, as measured with a plastic-gauge, was in the range of 0.147–0.158 mm for a 0.15 mm test gap size. Therefore, it was confirmed that the heating surface had sufficient wettability, and that the gap size was constant and sufficiently accurate with respect to the target value.

For the laser extinction method, a laser ray (3 mm diameter and 3.39 μm wavelength) was launched from a He–Ne laser emitter through the mini/micro-channel via a chopper, as shown in Fig. 3(c). A convex lens was used to focus the laser ray to a diameter of 0.6 mm. After passing through the convex lens and an optical filter, the laser ray was introduced to a Pb–Se detector with a light detection surface area of 3×3 mm^2.

The principle of the laser extinction method is to determine the micro-layer thickness, as illustrated in Fig. 4(a). The micro-layer thickness was determined using Lambert's law, as given in Eq. (1). The laser light extinction coefficient A is an unknown factor to be determined. Specifically, it was determined from the thickness δ of the test liquid and the transmittance ratio I/I_0 of the laser light by Utaka and Nishikawa [13]. I_0 and I denote the light intensities at the detector when the mini/micro-channel being measured is filled with steam and with a thin water layer and steam, respectively. δ and A are the micro-layer thickness and extinction coefficient, respectively.

$$\delta = -(1/A)\ln(I/I_0) \tag{1}$$

This method is sufficiently accurate to measure the micro-layer thickness of water on a micron scale inherently, because the values of I/I_0 are varied from 0.2 to 0.9 in relation to a range of 2 to 30 μm for the thickness of the micro-layer of water. Detailed investigation of the precision of the measurement of thin-liquid-layer thickness in Marangoni condensation phenomena was carried out by Utaka and Nishikawa [13]. The effects of ambient temperature change, reflection of laser ray etc. were examined on the values of I/I_0. As a result, it was shown that the error of measurement of thin liquid thickness was approximately ±0.3 m. Since the method to measure the micro-layer thickness in this study was almost same as Utaka and Nishikawa, it was applicable to this study.

The laser signals were recorded in synchronization with the process of bubble growth, which was recorded with a high-speed camera placed in front of the mini/micro-channel, as shown in Fig. 4(b). The relative location of the incident laser ray on the heating surface was adjusted to vary the distance from the incipient bubble.

3. Configuration of micro-layer in narrow gap mini/micro-channel boiling system

3.1. Effect of heat flux and distance from incipient bubble site on the initial micro-layer thickness

Heat flux and the distance from the incipient bubble site were examined as possible factors affecting the initial micro-layer thickness for the gap sizes of 0.15, 0.3 and 0.5 mm. The effect of heat flux on the initial micro-layer thickness for a gap size of 0.3 mm is shown in Fig. 5. Measurements were made at four different heat flux levels. No distinction in the initial micro-layer thickness was observed for different heat flux levels as similar to the cases of

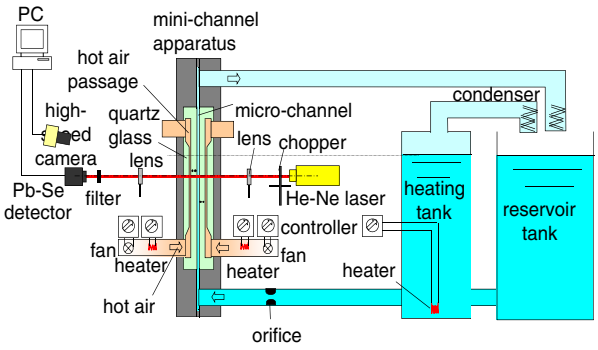

(a) Schematic of whole experimental system

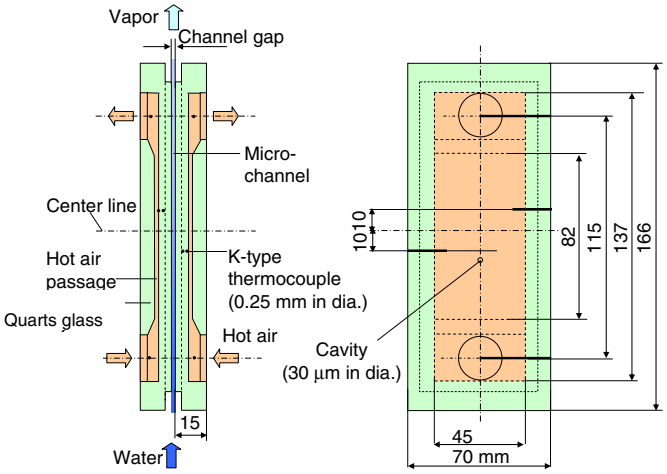

(b) Details of mini/micro-channel and heat transfer plate

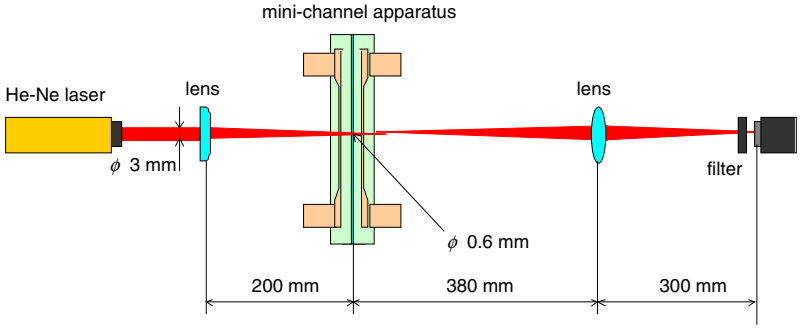

(c) Dimensions of laser system

Fig. 3. Experimental apparatus used for measuring micro-layer thickness.

0.15 and 0.3 mm gap sizes, indicating that the formation of the micro-layer is determined by the dynamic behavior of the liquid-vapor interface.

The effect of the distance from the bubble formation site on the initial micro-layer thickness for the gap size of 0.5 mm is shown in Fig. 6 for six different bubble forefront velocities. It was observed that the initial micro-layer thickness was weakly dependent on the distance from the bubble incipient site as similar to the cases of 0.15 and 0.3 mm gap sizes.

3.2. Effect of bubble forefront velocity and gap size on initial micro-layer thickness

The micro-layer is formed as a result of liquid remaining on the heating surface immediately after the liquid is pushed away by the bubble growth. The micro-layer thickness varies due to the effects of bubble forefront velocity and movement, and the evaporation rate from the micro-layer. Attention was focused on the initial micro-layer thickness δ_0 that appears immediately after the passage of the bubble forefront. It is thought that δ_0 is determined by the kinetic interface behavior in the process of bubble growth without being affected by evaporation of the micro-layer. On a highly wettable surface, the initial micro-layer thickness may depend on the effect of the two characteristic regions that are distinguished at a bubble forefront velocity of approximately 2 m/s (Fig. 5). Initial micro-layer thicknesses of between 2 and 28 μm were measured in the linear-increase region and approximately 18 μm in the constant thickness region for a gap size of 0.5 mm.

The variation of the initial micro-layer thickness in relation to the bubble forefront velocity is shown in Fig. 7 for three different

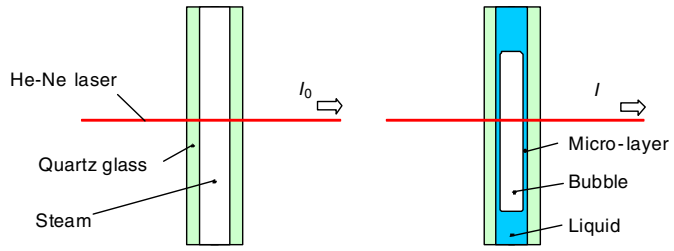

(a) Principle of laser extinction method for measuring micro-layer thickness

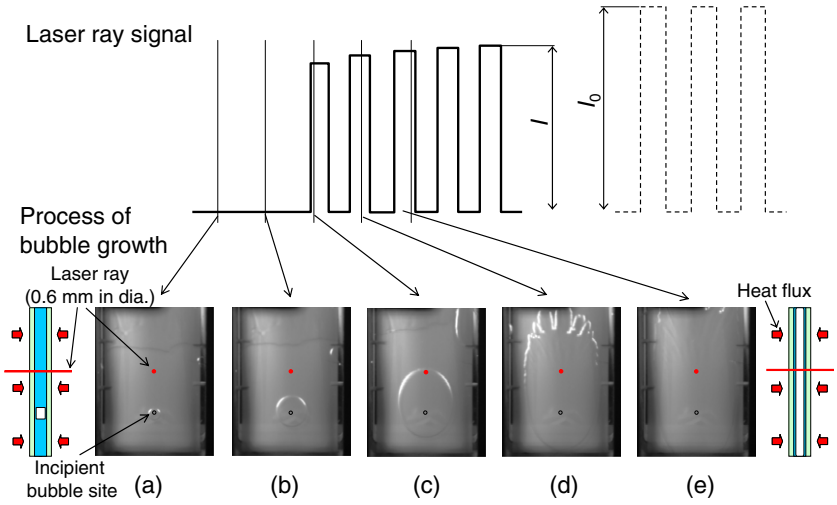

(b) Example of measuring process and aspect of bubble growth process

Fig. 4. Measurement method and example.

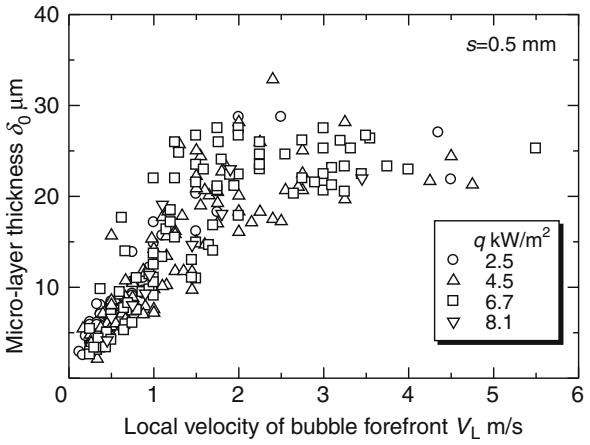

Fig. 5. Relationship between micro-layer thickness and bubble forefront velocity under different heat flux for a gap size of 0.5 mm.

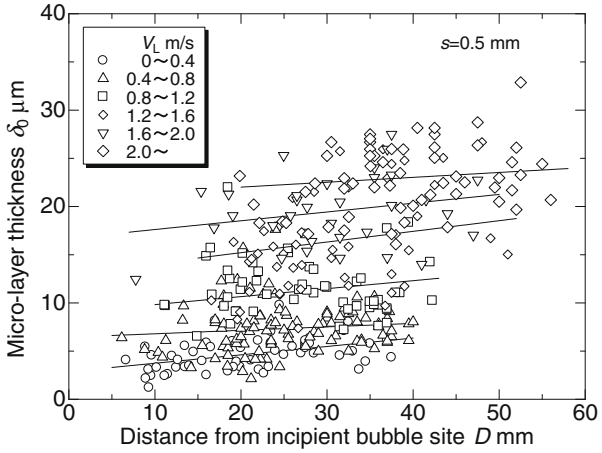

Fig. 6. Effects of distance from incipient bubble site and velocity of bubble forefront on initial micro-layer thickness.

mini/micro-channel gap sizes of 0.5, 0.3 and 0.15 mm. The tendency of the initial micro-layer thickness relative to the bubble forefront velocity for the different gap sizes changed at a bubble forefront velocity of 2.0 m/s. Moreover, the initial micro-layer thickness was strongly affected by the gap size, and decreased with decreasing gap size. In the constant thickness region, initial micro-layer thicknesses of 23, 18 and 9 μm were measured for gap sizes of 0.5, 0.3 and 0.15 mm, respectively.

These characteristics suggest that, for smaller gap sizes, the heat flux is larger in the low heat flux domain and the critical heat flux is lower than the dominant domain in the boiling curves. That is, in the micro-layer dominant region, the vaporization rate is increased, and higher boiling heat transfer is possible due to the thinner micro-layer. On the contrary, due to an increase in heat flux, the thinner liquid film disappears for a short time and a dryout region appears.

3.3. Distribution of initial micro-layer thickness

Fig. 8(a) shows the typical variations of bubble forefront velocity in relation to the distance, D, from the incipient bubble site at

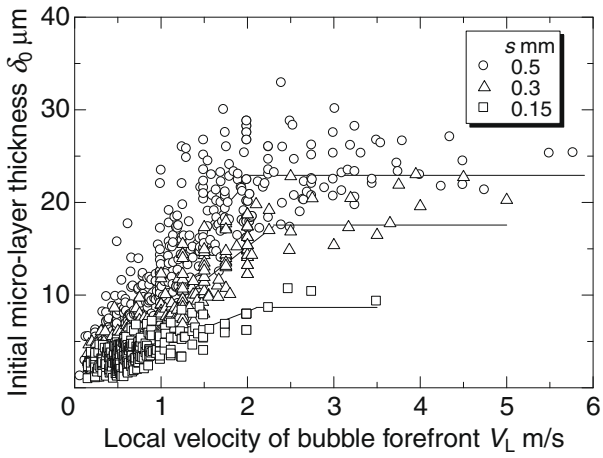

Fig. 7. Effect of bubble forefront velocity on initial micro-layer thickness for various gap sizes.

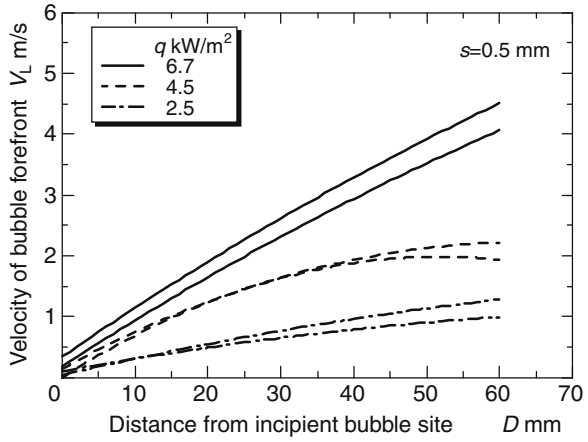

(a) Velocity of bubble forefront and distance from bubble incipient site

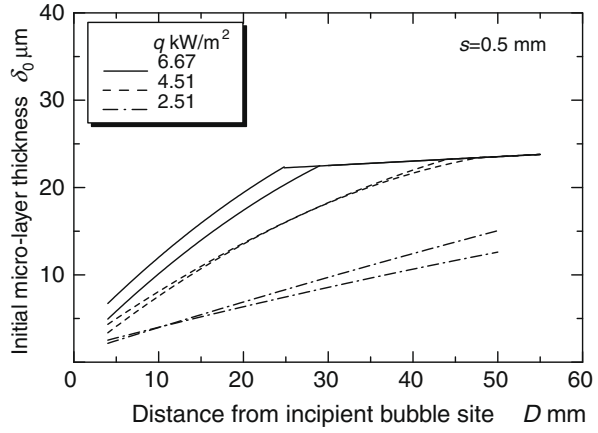

(b) Initial micro-layer thickness and distance from bubble incipient site

Fig. 8. Distribution of initial micro-layer thickness for $s = 0.5$ mm.

three different heat fluxes and a gap size of 0.5 mm. As a bubble grows and enlarges, the velocity of the bubble forefront increases. Fig. 8(b) shows the distributions of initial micro-layer thickness on the heating surface, derived from the relation between the bubble forefront velocity and the distance from the bubble formation site, as shown in Figs. 6 and 7. The initial micro-layer thickness increases, because the bubble forefront velocity increases with increasing heat flux; and the initial micro-layer thickness is between 1–2 and 10–20 μm, in the region of D between 3 and 50 mm, respectively. Furthermore, the initial micro-layer thickness increases with increasing D, which corresponds to the tendency for the bubble forefront velocity to increase, as shown in Fig. 7. The initial micro-layer thickness increases monotonically in the lower heat flux region in which the bubble forefront velocity is out of the region of constant micro-layer thickness. On the other hand, as the heat flux increases, a constant thickness appears in the region of larger D. The initial micro-layer thickness becomes constant at smaller D with increasing heat flux.

4. Consideration of heat transfer characteristics on the basis of configuration of micro-layer

4.1. Characteristics of phenomena in micro-layer dominant region and method of analysis of heat transfer characteristics

A micro-layer dominant region described in the explanation concerning Fig. 2 is the principal form of heat transfer in narrow gap mini/micro-channel boiling. Therefore, the heat transfer characteristics are discussed using various characteristics of the liquid micro-layer thickness elucidated in Section 3, and heat transfer measurement data and analysis of images taken, for the micro-layer dominant region reported in Ref. [11]. The measuring system used in Ref. [11] is basically the same as that used in this study; therefore, the results of the heat transfer and liquid micro-layer measurements are comparable.

The micro-layer dominant region consists of a liquid saturation period where the whole gap is filled with the liquid and a micro-layer period where the vapor bubble is formed in the gap and a micro-layer exists on the heat transfer surface underneath the vapor bubble. These two periods are repeated alternately. The micro-layer period can be classified into two phases: an initial liquid micro-layer that is formed on the heat transfer surface by bubble generation and growth from the liquid saturation period, and a reformed liquid micro-layer that is formed again by the transfer of a liquid slug accompanying the dynamic and complicated behavior of bubbles.

To study the evaporation mechanism and heat transfer characteristics in the micro-layer dominant region, the mini/micro-channel boiling phenomenon is modeled as described below. In order to investigate the effect of micro-layer evaporation qualitatively, the heat flux is assumed to be constant. Since such a heating condition in calculation are different from that in experimental system due to the presence of heat transfer plate, further investigation will be required for more detailed study.

(1) The bubble generation cycle is the sum of the liquid saturation period t_L and the micro-layer period t_M.
(2) The micro-layer period consists of an initial micro-layer and a reformed micro-layer.
(3) Bubbles are generated at a constant site that is a function of the heat flux.
(4) The bubble growth rate is another function of the heat flux.
(5) The averaged values during the period of measurement were used for the above mentioned factors such as the bubble generation cycle, liquid saturation period, micro-layer period, initial micro-layer period, reformed micro-layer period, incipient bubble site, and bubble growth rate all data throughout during the period of measurement is averaged.

For the heat transfer surface indices, average values were measured at a total of nine representative reading positions, as shown in Fig. 9: three non-dimensional positions (x^* = 0.20, 0.50, 0.80) from upstream to downstream of the heat transfer surface with height H = 102 mm and three non-dimensional positions (y^* = 0.22, 0.5, 0.78) in the span direction width W = 50 mm, as used for heat transfer measurements in Ref. [11]. Since every index showed a small difference in the y^* direction, the averages in the y^* direction were adopted by taking the x^* direction into consideration.

4.1.1. Determination of the incipient bubble site and the bubble front velocity

Figs. 10 and 11 show the changes of the average incipient bubble site for each average heat flux determined from high-speed images, and the changes of the mean bubble forefront velocities generated from these sites, respectively. In Fig. 10, symbol ○ represents the measured position of incipient bubble sites and ● represents the average position. At each heat flux, the changes in the positions of the incipient bubble site are limited to a comparatively narrow range. This justifies the validity of averaging. The curves in Fig. 11 show the averages of 5–10 patterns of bubble forefront velocity as determined from the images under each heat flux condition. The bubble forefront velocity V_L tends to increase monotonically as the distance and heat flux increases.

The bubble forefront velocity V_L at distance D from the incipient bubble point can then be calculated. By applying these values to the results shown in Fig. 6, the initial micro-layer thickness δ_0, at each position x^* in the micro-layer period, can be obtained, where the value at an arbitrary bubble forefront velocity is determined by interpolation.

4.1.2. Determination of the liquid saturation period t_L and the micro-layer period t_M

The liquid saturation period and the micro-layer period were measured as a time series throughout the image capturing period. Fig. 12 shows the relationship between the average heat flux, and the average liquid saturation period t_L and liquid micro-layer period t_M at three x^* positions. As x^* increases, the liquid saturation period becomes shorter and the micro-layer period becomes longer. As the heat flux increases, the liquid saturation period becomes remarkably shorter and the micro-layer period becomes longer. As mentioned in Section 4.1.1, this indicates that the incipient bubble site x^* grows with a decrease in heat flux and the bubbles generated tend to extend upward by the effect of gravity.

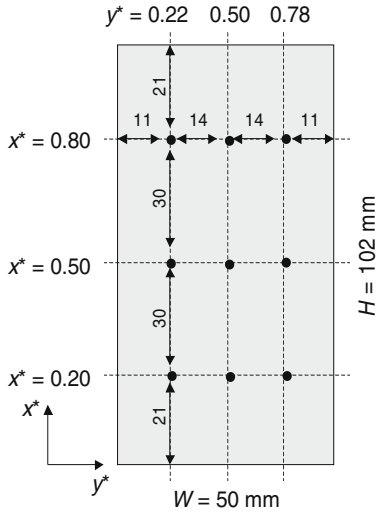

Fig. 9. Measurement positions on the heat transfer surface.

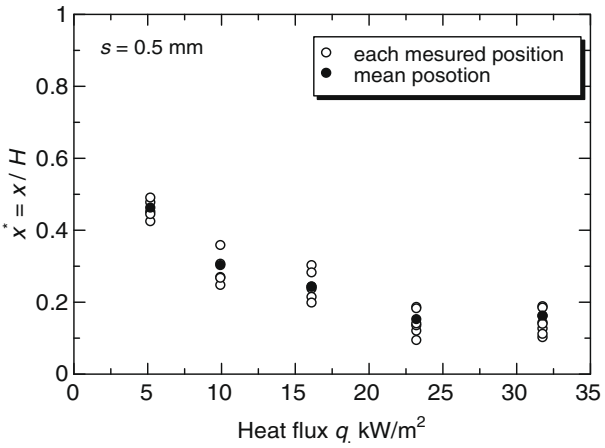

Fig. 10. Positions of the incipient bubble site.

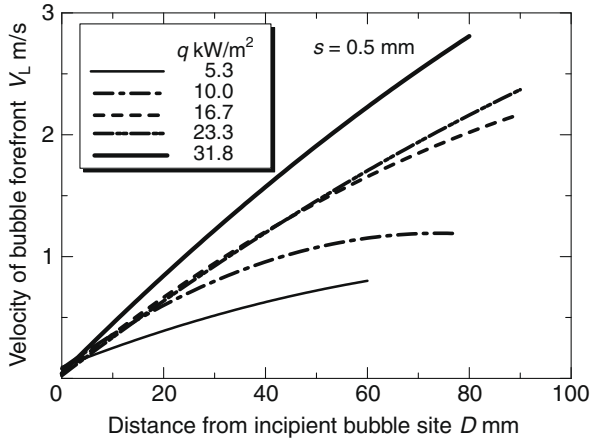

Fig. 11. Mean bubble forefront velocity and the distance from the incipient bubble site.

4.1.3. Ratio of micro-layer reformation in the liquid micro-layer period

The liquid micro-layer period consists of both initial and reformed micro-layers. It is necessary to determine the number of micro-layers reformed by the movement of liquid slugs in a single liquid micro-layer period. From the experimental images, the number of initial micro-layers formed by bubble growth, and the number of micro-layers reformed by later liquid slug movement were determined and their ratio was calculated, as shown by Eq. (2)

$$\frac{N_R}{N_B} = \frac{\text{number of times of micro-layer re-apperance by liquid slug}}{\text{number of times of initial micro-layer apperance by bubble growth}}. \quad (2)$$

Both the initial and reformed liquid micro-layers were equally dependent on the determining factors of micro-layer-thickness, with no discrepancy between them. Fig. 13 shows the measured results. In the region of small heat flux, the number of reformed micro-layers is very small. However, as the heat flux increases, the movement of the liquid slug becomes active and the frequency of micro-layer reformation increases. At the upstream where x^* is small, micro-layers are hardly reformed. However, as x^* increases, the frequency of reformed micro-layers increases.

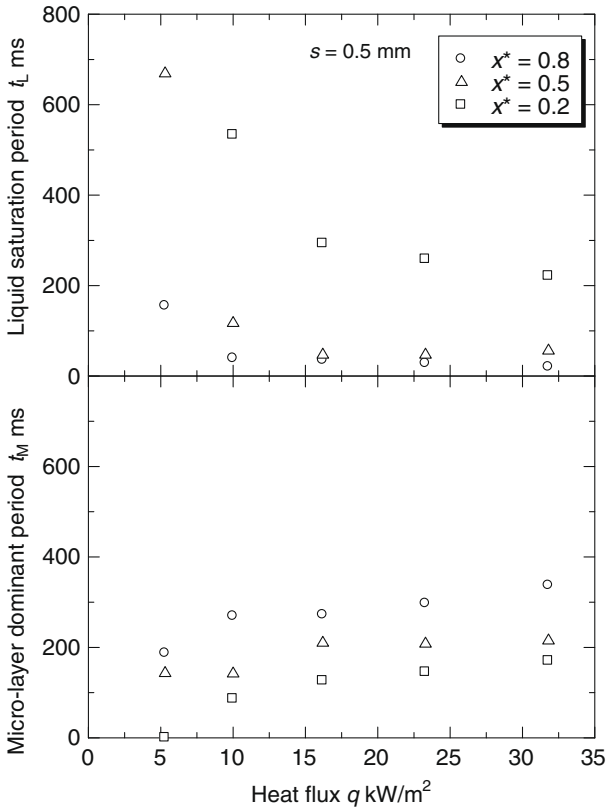

Fig. 12. Heat flux vs. the liquid saturation and micro-layer periods.

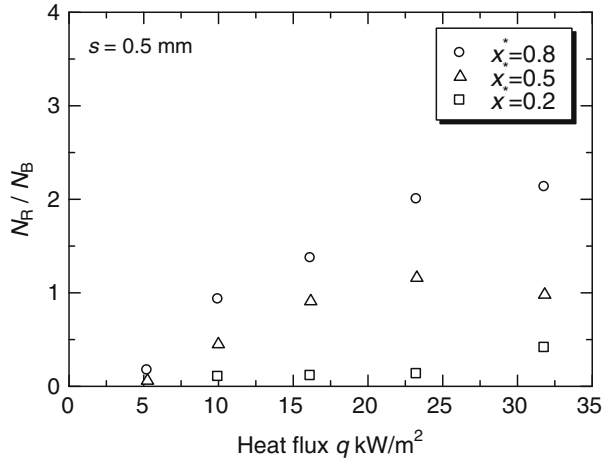

Fig. 13. Relationship between average heat flux and N_R/N_B.

4.1.4. Calculation of the micro-layer thickness and the degree of surface superheat

To study the heat transfer characteristics where a liquid micro-layer is formed, the variation of the liquid micro-layer thickness and the degree of superheat in the bubble generation cycle were determined as follows.

4.1.4.1. Micro-layer period. In the micro-layer period, steady-state heat conduction by the micro-layer, which is dependent on the wall temperature T_W and the saturation temperature T_0, and causes liquid to evaporate at constant heat flux, so that the micro-layer loses thickness δ is reduced from the initial micro-layer thickness δ_0. This is also same to the reformed liquid micro-layer. Using Eqs. (3)–(5), the changes in the micro-layer thickness during the micro-layer period, and the transition of the degree of superheat on the heat transfer surface were calculated,

$$v = \frac{q}{\rho_L L} \tag{3}$$

$$\delta = \delta_0 - vt \tag{4}$$

$$\Delta T = T_W - T_0 = q\frac{\delta}{\lambda} \tag{5}$$

4.1.4.2. Liquid saturation period. Fig. 14 shows a model of the liquid saturation period. Immediately after vapor bubbles pass, the gap is filled with water at saturation temperature, and is heated from the heat transfer surface at constant heat flux. The surface facing the gap side of the heat transfer surface is thermally insulated. The liquid moves comparatively slowly, so that only heat conduction is considered in regard to the temperature changes in the liquid. By solving the one-dimensional equation of heat conduction in unsteady state Eq. (6), under the initial conditions Eq. (7), and boundary conditions Eq. (8), the degree of superheat is calculated

$$\frac{\partial T}{\partial t} = \alpha\frac{\partial^2 T}{\partial z^2} \tag{6}$$

Initial conditions:

$$\begin{cases} T = 0 : T = T_{WE} \quad (z = 0) \\ T = T_0 \quad (0 \le z \le s) \end{cases} \tag{7}$$

Boundary conditions:

$$\begin{cases} z = 0 : -\lambda\dfrac{\partial T}{\partial z} = q \\ z = s : \dfrac{\partial T}{\partial z} = 0 \end{cases} \tag{8}$$

4.2. Analysis and discussion of the heat transfer characteristics

Using the method shown above, the analysis was performed for a gap of 0.5 mm with five patterns of heat flux. As an example, Fig. 15(a–c) shows the transitions of the micro-layer thickness, and the degree of surface superheat during a cycle of bubble generation at $x^* = 0.20$, 0.50 and 0.80, respectively, for a heat flux of 31.8 kW/m^2. In the liquid saturation period, the degree of superheat increases over time. Once the micro-layer is formed, the degree of superheat drastically decreases. As evaporation reduces the thickness of the micro-layer, the degree of superheat is gradually decreased further. The micro-layer period can be divided into several periods. Between the divided periods, there are also periods of several milliseconds in duration where the micro-layer thickness increases. These periods are attributable to the quick passage of a liquid slug. In Fig. 15, different results are given for each x^* on the right and left. This is because the value of the micro-layer reformation ratio N_R/N_B from Eq. (1) does not generally become an integer, and therefore those micro-layer reformations counted with a difference of one were divided right

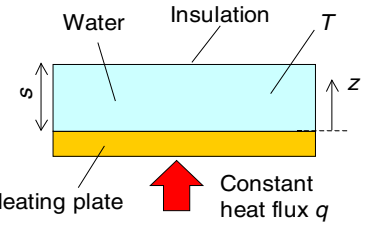

Fig. 14. Calculation model for the liquid saturation period.

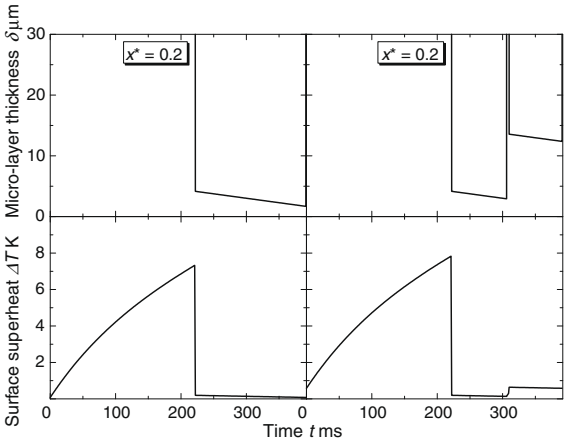

(a) $x^* = 0.2$

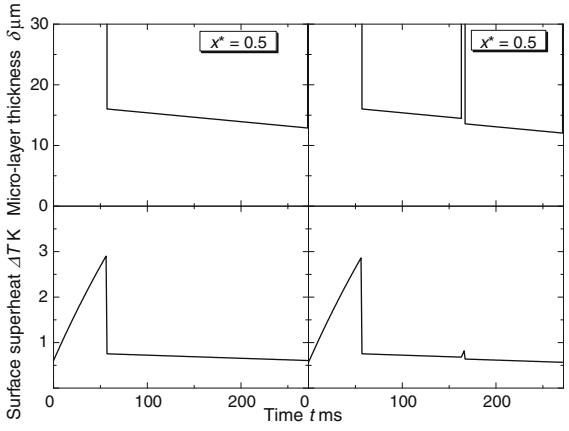

(b) $x^* = 0.5$

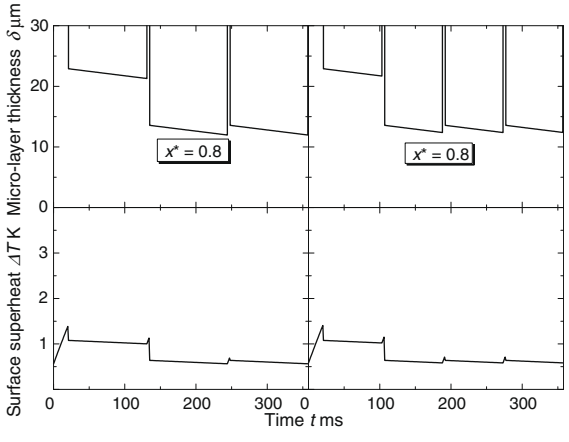

(c) $x^* = 0.8$

Fig. 15. Variations of micro-layer thickness and surface superheating in the vapor bubble cycle for $s = 0.5$ and $q = 16.2$ kW/m^2.

way. For example, when the micro-layer reformation ratio is greater than 0, but smaller than 1, bubble generation cycles with no micro-layer reformation and those with single micro-layer reformation coexist, and are therefore divided according to the ratio. With regard to the reformed micro-layer thickness in the cycles, the movement velocities of liquid for micro-layers reformed by the movement of liquid slugs were mostly distributed from 0.8 to 1.6 m/s at every heat flux in this experiment. Consequently, the initial liquid micro-layer thickness of reformation is calculated to be approximately 10–16 μm. The reformed micro-layer thickness is distributed narrow range; therefore, a constant value of 13.6 μm, averaged from all data, was adopted as the reformed micro-layer thickness. The other conditions were also equally determined.

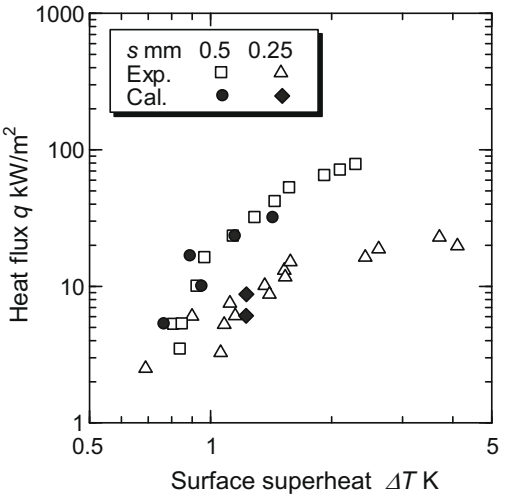

Fig. 16. Comparison between experimental and calculated boiling curves.

Fig. 16 shows the results of calculating the average degree of superheat at each heat flux for the gap sizes of 0.5 and 0.25 mm, and comparing the calculated results with the experimentally obtained boiling curve in Ref. [11]. In Fig. 16, symbols □ and △ represent experimentally obtained results, and ● and ♦ represent calculated values. The calculated values are in good agreement with the experimental results. This confirms that an evaporation rate can be predicted using the micro-layer thickness; that the micro-layer dominant region, the principal form of narrow gap mini/micro-channel boiling, is determined by the liquid saturation period constituting a bubble generation cycle, and a micro-layer period where the micro-layer evaporates. In addition, it was confirmed that the heat transfer was enhanced due to the micro-layer evaporation and the low degree of superheat in the micro-layer period, which occupied a comparatively long duration, indicates good heat transfer in the micro-layer dominant region.

5. Conclusions

The thickness of the micro-layer that forms on a heating surface by vapor growth was measured using the laser extinction method for mini/micro-channel gap sizes of 0.5, 0.3 and 0.15 mm, in order to clarify the heat transfer characteristics of boiling in a mini/micro-channel vapor generator. Furthermore, the heat transfer characteristics in narrow gap mini/micro-channel boiling were investigated for the micro-layer dominant region. The following results were obtained for mini/micro-channel gap sizes of 0.5, 0.3 and 0.15 mm.

(1) The initial micro-layer thickness was determined by the gap size and the velocity of the bubble forefront.
(2) The trend in the variation of the micro-layer thickness, relative to the velocity of the bubble forefront, is divided into two regions; from the low velocity side, a region where the thickness increases linearly with increasing velocity, and a region where the thickness is almost constant. The boundaries of the two regions were determined at a bubble forefront velocity of 2 m/s.

(3) The initial micro-layer thickness decreases with the decreasing gap size of the mini/micro-channel. The initial micro-layer thickness was approximately 1–2 μm in the region of linear increase. In the constant thickness region, the micro-layer thickness values were 8–24 μm for a mini/micro-channel gap size in the range of 0.15–0.50 mm.
(4) The initial micro-layer thickness increases due to an increase in the bubble forefront velocity with increasing heat flux. The distribution of initial micro-layer thicknesses of between 4 and 24 μm on the heating surface is in the region of distance, D, between 10 and 60 mm.
(5) On the basis of the measured characteristics of the micro-layer, the factors analyzed, that is, (a) the position of incipient bubble site, (b) the bubble forefront velocity against the distance from the bubble site, (c) the terms of liquid saturation and micro-layer formation, and (d) the ratio between numbers of initial micro-layer appearances by bubble growth and by a formation of liquid slug were measured and their characteristics were clarified.
(6) Prediction of the vaporization rate was confirmed by applying the measured micro-layer thickness and the factors outlined in (5) above. Further, it was confirmed that the heat transfer was enhanced due to the micro-layer evaporation.

Acknowledgment

This work was partially supported by a Grant-in-Aid for Scientific Research of the Ministry of Education, Culture, Sports, Science and Technology, Japan [(B)(2)17360096].

References

[1] S.S. Mehendale, A.M. Jacobi, Evaporative heat transfer in mesoscale heat exchangers, ASHRAE Trans. 106 (1) (2000) 446–452.
[2] S.G. Kandlikar, Two-phase flow patterns, pressure drop and heat transfer during boiling in mini-channel and micro-channel flow passages of compact evaporators, Heat Transfer Eng. 23 (2002) 5–23.
[3] D.S. Wen, Y. Yan, D.B.R. Kenning, Saturated flow boiling of water at atmospheric pressure in a 2 mm × 1 mm vertical channel: time-averaged heat transfer coefficients and correlations, in: Proceedings of 8th UK National Heat Transfer Conference, 2003.
[4] J.R. Thome, V. Dupont, A.M. Jacobi, Heat transfer model for evaporation in microchannels. Part I: presentation of the model, Int. J. Heat Mass Transfer 47 (2004) 3375–3385.
[5] V. Dupont, J.R. Thome, A.M. Jacobi, Heat transfer model for evaporation in microchannels. Part II: comparison with the database, Int. J. Heat Mass Transfer 47 (2004) 3387–3401.
[6] Y. Katto, S. Yokoya, Experimental study of nucleate pool boiling in case of making interference plate approach to the heating surface, Proc. 3rd Int. Heat Transfer Conf. 3 (1966) 219.
[7] Y. Fujita, H. Ohta, S. Uchida, Heat transfer in nucleate boiling within a vertical narrow space, JSME Int. J. Ser. II 31 (3) (1988) 513.
[8] M.G. Cooper, A.J.P. Lloyd, The microlayer in nucleate pool boiling, Int. J. Heat Mass Transfer 12 (1969) 895–913.
[9] P. Stephan, Microscale evaporative heat transfer: modeling and experimental validation, in: Proceedings of 12th International Heat Transfer Conference, 2002.
[10] P.C. Wayner Jr., Intermolecular forces in phase-change heat transfer: Kern award review, AIChE J. 45 (10) (1999) 2005–2068.
[11] Y. Tasaki, Y. Utaka, Effects of surface properties and gap sizes on boiling heat transfer characteristics in a micro-channel vapor generator, J. Enhanced Heat Transfer 13 (3) (2006) 245–260.
[12] Y. Utaka, T. Nishikawa, Measurement of condensate film thickness for Solutal Marangoni condensation applying laser extinction method, J. Enhanced Heat Transfer 10 (2) (2003) 119–129.
[13] Y. Utaka, T. Nishikawa, An investigation of liquid film thickness during Solutal Marangoni condensation using laser absorption method: absorption property and examination of measuring method, Heat Transfer – Asian Res. 30 (8) (2003) 700–711.